

Design of a high-resolution VLS monochromator for synchrotron radiation

© A.N. Shatokhin,¹ E.A. Vishnyakov,¹ A.O. Kolesnikov,¹ A.D. Nikolenko,^{2,3} E.N. Ragozin¹

¹ Lebedev Physical Institute, Russian Academy of Sciences,
119991 Moscow, Russia

² Budker Institute of Nuclear Physics, Siberian Branch, Russian Academy of Sciences,
630090 Novosibirsk, Russia

³ Borekov Institute of Catalysis, Siberian Branch of RAS,
630090 Novosibirsk, Russia

e-mail: shatohinal@gmail.com

Received March 29, 2021

Revised March 29, 2021

Accepted March 29, 2021

A high-resolution monochromator with a broad spectral range of 125–4200 Å is designed for a measuring beamline of the projected synchrotron radiation source „SKIF“ (Novosibirsk). The optical configuration of the monochromator comprises a grazing-incidence concave mirror, a plane VLS grating, and an exit slit. It is planned to use two replaceable VLS gratings with central groove frequencies of 600 and 150 mm⁻¹ intended for subranges of 125–1000 Å and 900–4200 Å, respectively. Wavelength tuning in each of the two subranges is carried out by solely the rotation of the VLS-gratings. Due to the proper choice of p_1 VLS-grating coefficients, the focal distance varies only slightly over the entire spectral range, and the p_2 VLS-grating coefficients are used to suppress the aberrations of the mirror and the gratings. The resolving power of the configuration obtained by numerical ray tracing exceeds 1000 in the 125–1000 Å range and 2000 in the 900–4200 Å range.

Keywords: VUV, spectroscopy, VLS-grating, synchrotron radiation.

DOI: 10.21883/TP.2022.13.52230.86-21

Introduction

The Siberian ring source of photons „SKIF“ is a 4th generation source of synchrotron radiation, intended for a wide range of works using X-ray and vacuum ultraviolet (VUV) radiation to the benefit of various branches of science and technology. As expected, the complex will be commissioned in 2024. At the first stage of the source operation, it comprises six synchrotron radiation end stations, most of which are devoted to hard X-ray radiation. Only one of the six stations of the first stage (station 1-6, „Electron structure“, [1]) will be focused on the usage of soft X-ray and VUV radiation in the 10–2000 eV spectral range. This station capacity will be not enough to cover experimental needs in the area of VUV and soft X-ray range, therefore the corresponding stations should be provided in the second stage. Due to the predictable lack of experimental capacities at the first stage, the station 1-6 was designed as the unit with maximum broad spectral coverage. For second stage stations it is reasonable to reduce spectral coverage of each of the new stations by means of improving other consumer characteristics. Thus, among second stage stations at least one VUV-range station is provided for operation in spectral range of 3–100 eV, that, in comparison with the station 1-6, will have bigger acceptance, and, as a result, allow to obtain bigger photon flux in its operational spectral range. It is expected that this station will receive radiation from the synchrotron bending magnet and will be devoted to study of various objects ignition kinetics with the usage of

mass spectrometry with photon ionization of the combustion products. In addition several metrological techniques for various consumers are expected to be implemented at this station. We propose a monochromator designed for use at this station.

Cutting-edge researches, performed at third and fourth generation synchrotrons, often require high spectral purity monochromatic radiation forming out, as well as quickness and convenience of radiation channel reconfiguration to another wavelength. When using high resolution grating monochromator for VUV spectral range monochromatic radiation forming out of polychromatic beam of synchrotron radiation (SR), it is extremely preferable to keep the monochromator focal distance and the direction of diffracted radiation constant at operational wavelength reconfiguration. In this case the position of the exit slit remains unchanged and the number of element transfers in vacuum is minimized. This task can be solved, first of all, in the modified Cherny–Turner scheme with application of a plane reflecting grating, operating in parallel beam, and two grazing-incidence concave mirrors (preferably off-axis parabolic/elliptic cylinders), intended for collimation and the following radiation focusing [2]. Secondly, this task is solved in Hettrick–Underwood scheme using a focusing mirror and a plane VLS grating,¹ operating in a convergent beam [3,4]. Both schemes are simple: the wavelength

¹ Reflecting gratings with groove density, that monotonically changes across the aperture as per desired law, are called VLS gratings (Varied Line-Space Gratings).

is reconfigured by means of rotation of the grating only. However, in the Hettrick–Underwood VLS monochromator scheme there are only two optical elements used, and high and ultra-high ($\lambda/\delta\lambda > 10^4$) resolving power achieving is not associated with grazing-incidence aspheric optics use.

It should be noted that there are other optical schemes of high-resolution monochromators with a fixed exit slit, that maintain the output direction of the diffracted radiation (see, for instance, [5]). In [5] there were used a cylindrical mirror, a plane grating and an auxiliary plane mirror, while the wavelength scanning was performed by the grating rotation, coordinated with rotation and simultaneous translation of the plane mirror. Disadvantage of such schemes is the large number of optical elements, as well as certain difficulties with reconfiguration of operational wavelength. Examples of schemes of devices with complex kinematics of optical elements can be found in reviews, for instance, [6,7].

Currently VLS spectrometers and VLS monochromators of various type are widely used in researches in soft X-ray (SX) spectral range [6,7]. They are used in spectroscopy and diagnostics of laboratory plasma [8], astrophysics [9–11], reflectometry/metrology with usage of laser plasma SX radiation source [12], X-ray fluorescent analysis with usage of SR and emission spectroscopy combined with electron microscope [13]. User channels for SX/VUV radiation at foreign synchrotrons are often equipped with monochromators and spectrometers based on VLS gratings [14–16]. Special VLS spectrometers for investigation of the electron structure of various materials and molecules using the spectroscopic method of resonant inelastic X-ray scattering (RIXS) under SR operation are actively developed [17–19].

The capability of gratings with monotonically changing groove density (to modify the spectral focal curve) was noted by M. Cornu back in 1893 [20]. However after that, almost throughout the century, the efforts of gratings manufacturers were focused on maintaining the maximum equidistance of grooves, since it was associated with high quality of gratings. In 1970–1980s T. Harada [9,21–24], M. Hettrick and J. Underwood [3,4,25] focused toward the idea of using the focusing properties of aperiodic gratings. Scanning spectrometers/monochromators with plane VLS grating (Hettrick spectrometers) became widespread and commercially available [25]. Today there are programmable engraving machines, interference lithography and electron beam lithography as methods for the VLS gratings manufacturing (see reviews [6,7]).

Over the last years the technology of plane and concave VLS gratings production using the interference lithography method, including calculation of interference lithography optical scheme, was developed in Russia and experience in VLS spectrometers manufacturing was accumulated [6,7,26,27]. Considering this, as well as wide possibilities of Hettrick-Underwood approach, we chose this paradigm for calculation of the VLS monochromator scheme for the VUV channel at the 4th generation synchrotron device „SKIF“.

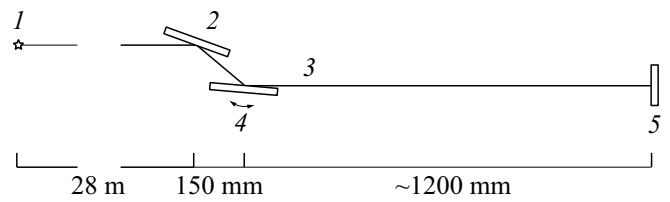


Figure 1. Schematic of the monochromator based on a plane VLS grating: 1 — source, 2 — concave mirror, 3 — replaceable VLS grating, 4 — wavelength reconfiguration is performed by simple grating rotation, 5 — exit slit.

1. Problem Statement

We propose VLS monochromator for SR within a spectral range of 125–4200 Å based on a grazing-incidence plane VLS grating, operating in a convergent beam. Specifics of SR channel set the scheme geometry: distance from deflecting synchrotron magnet to monochromator optical elements is constant and equals to ~ 28 m; optical elements should be densely located; distance from optical elements to exit slit is also constant and equals to ~ 1200 mm; output direction of the radiation after the slit should also be constant. The preferred resolving power should be $\lambda/\delta\lambda > 10^3$ over the whole spectral range.

The following scheme is used for the monochromator (Fig. 1). Radiation from a practically point source is focused by a grazing-incidence concave spherical mirror, while horizontal focus of the beam is on the distance, almost equal to the distance to exit slit. The mirror mounting is very different from the Rowland one and is strongly asymmetrical. After the mirror, the convergent beam is incident on the plane VLS grating and then diffracted into the first external order. For usage convenience, the scheme does not deflect the incoming radiation: angle of deflection by the grating is equal in value and opposite in sign to the angle of deflection by the mirror. Due to the VLS grating properties, the radiation is focused around the plane of the exit slit, and wavelength change is performed only by means of a simple grating rotation. Spectrometer scheme is similar to Hettrick-Underwood scheme [3,4], but differs from it with strongly asymmetrical mounting of the focusing mirror.

2. Scheme calculation

Let's discuss a simple diffraction grating with grooves frequency dependency $p(w)$, where w stands for the coordinate on the grating aperture, perpendicular to the grooves (Fig. 2).

Let's expand this law in Taylor series in coordinate w : $p(w) = p_0 + p_1w + p_2w^2 + \dots$. Here p_0 is the frequency of the grooves in the aperture center, and this coefficient is responsible for the direction of the diffracted radiation, while coefficient p_1 is responsible for focusing properties

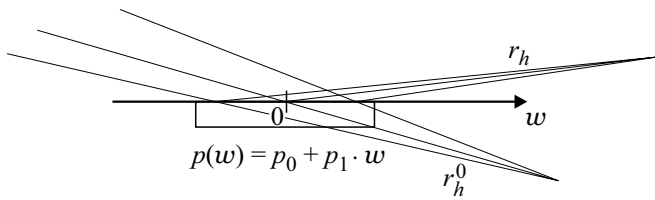


Figure 2. Changing the focal distance after diffraction on a plane reflecting VLS grating.

of the grating, and coefficient p_2 can compensate the meridional coma aberration of the diffracted beam [26].

Let a parallel monochromatic beam with a wavelength λ_1 impinge on this grating at a grazing angle φ_1 and then diffract into the order m at a grazing angle ψ_1 . Then the values are related by the equation of the diffraction grating (1):

$$\cos(\psi_1) - \cos(\varphi_1) = mp_0\lambda_1. \quad (1)$$

With the same position of the incident and diffracted beams, let's rotate the grating by a small angle. Now let the parallel monochromatic beam with a wavelength λ_2 impinge on the grating at a grazing angle φ_2 and diffract into the order m at a grazing angle ψ_2 , while $\varphi_1 + \psi_1 = \varphi_2 + \psi_2 = \Omega$. Thus, the reconfiguration of the wavelength is performed under the constant direction of the incoming and diffracted radiation. Relation between the wavelength and the angle of incidence of the radiation onto the grating is defined by the formulas

$$\varphi = \frac{\Omega}{2} - \arcsin \frac{mp_0\lambda}{2 \sin(\Omega/2)},$$

$$m\lambda = \frac{2 \sin(\Omega/2) \sin(\Omega/2 - \varphi)}{p_0}. \quad (2)$$

Such a scheme settles a query of constant direction of the incoming and the diffracted radiation. To solve the problem of a constant focal distance for the diffracted radiation, we will use the properties of the VLS gratings.

Let the convergent beam with a wavelength λ and a distance from the grating center to the focus r_h^0 fall onto the grating (Fig. 2). Then the diffracted radiation will focus at the distance r_h , defined by the formula (3):

$$m\lambda p_1 = \frac{\sin^2 \varphi}{r_h^0} - \frac{\sin^2 \psi}{r_h}. \quad (3)$$

If we insist of fulfilling of this condition for two wavelengths $\lambda_{1,2}$ with the same p_1 and r_h , in the scheme with grating rotation, described earlier, then we receive a strict limitation for r_h (4):

$$r_h = r_h^0 \frac{\sin^2 \psi_1 \lambda_2 - \sin^2 \psi_2 \lambda_1}{\sin^2 \varphi_1 \lambda_2 - \sin^2 \varphi_2 \lambda_1}. \quad (4)$$

Also p_1 is no longer a free parameter (5):

$$p_1 = \left(\frac{\sin^2 \varphi_1}{r_h^0} - \frac{\sin^2 \psi_1}{r_h} \right) / \lambda. \quad (5)$$

I.e. when using a VLS grating, which coefficient p_1 meets (5), and angle of grazing incidence onto the grating meets (2), we receive that the focal distance is the same (r_h) for grazing angles $\varphi_{1,2}$ and their corresponding wavelengths $\lambda_{1,2}$, while the output direction of the radiation is the same for all wavelengths.

3. Selection of scheme parameters

Due to the wide bandwidth of the required spectral range (125–4200 Å), when using a single diffraction grating in the monochromator scheme the defocusing will be significant at any selection of a pair of wavelengths $\lambda_{1,2}$. Therefore, our scheme assumes using two replaceable diffraction gratings.

Roughly equal on a logarithmic scale ranges 125–1000 Å and 900–4200 Å are proposed as the two ranges. Angle of 32°, corresponding to an angle of radiation grazing

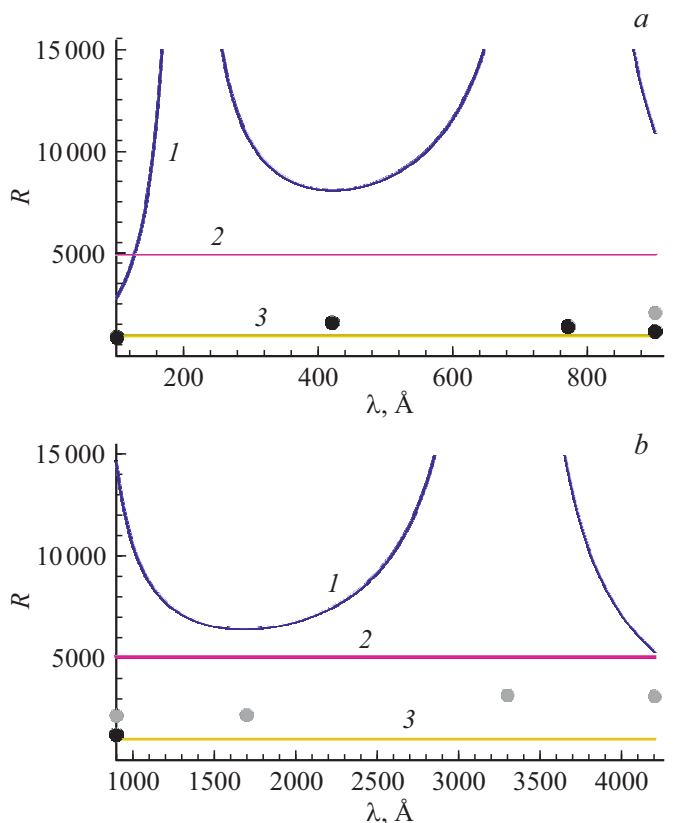


Figure 3. 1 — calculated dependence of the monochromator resolving power against the wavelength, considering only geometrical defocusing (without considering the aberrations) for two VLS gratings (ranges 125–1000 Å (a) and 900–4200 Å (b)); 2 — resolving power, corresponding to 5000, 3 — resolving power, corresponding to 1000. Dots show the resolving power calculated using numerical ray tracing (considering aberrations).

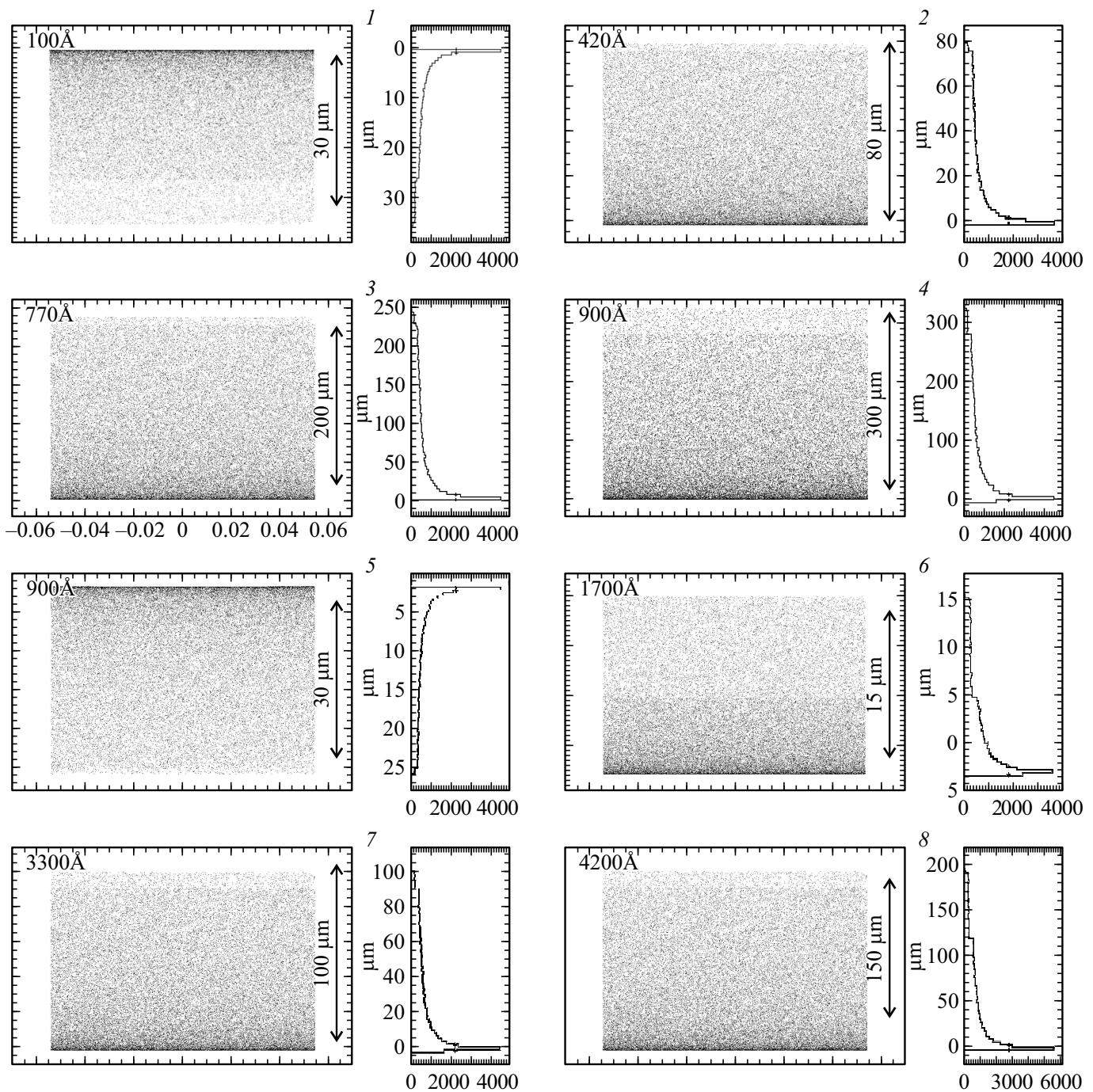


Figure 4. Spectral images of the monochromatic point source, obtained by the numerical ray tracing method for two VLS gratings (ranges 125–1000 Å (upper) and 900–4200 Å (lower)).

onto the mirror of 16° , is selected as an angle of deflection by the grating (and the mirror). At such radiation grazing-incidence angle the gold coating of the mirror reflects more than 45% of radiation energy in the whole required spectral range. This angle is a parameter of scheme optimization. This angle reduction results in increase of the mirror and the grating reflection coefficient, but also in decrease of the resolving power

and acceptance angle of the device. 600 and 150 mm^{-1} are selected as an average groove frequency of VLS gratings.

For selection of monochromator scheme its parameters should be optimized as per certain criteria. The resolving power of the device in the whole required spectral range is selected as one of these criteria. The resolving power is defined by the source image width in the plane of the

Monochromator parameters

Concave mirror			
Curve radius, mm		9356	
Aperture D , mm		50	
Incidence angle, °		74	
Source-mirror distance, mm		28000	
Mirror-focus distance, mm		1352	
Mirror-VLS grating distance, mm		150	
Flat VLS grating			
Aperture, mm		50 × 20	
Deflection angle, °		32	
Diffraction order		The first external	
Grating-exit slit distance, mm		1200	
Spectral range, Å		125–1000	900–4200
Coefficients VLS gratings	p_0, mm^{-1}	600	150
	p_1, mm^{-2}	0.956	0.239
	p_2, mm^{-3}	$-1.6 \cdot 10^{-3}$	$-1.4 \cdot 10^{-3}$
Inverse linear dispersion, Å/mm		3.6–2.3	14–9.1
Resolving power		> 1000	> 2000

exit slit S and inverse linear dispersion (plate scale) of the device $d\lambda/ds$ through correlation $\lambda/\delta\lambda = \lambda/(Sd\lambda/ds)$. Image width is composed of geometrical defocusing S_g , higher-order aberrations S_a and diffraction divergence S_d . As the criteria of successful optimization of the scheme let's take the resolving power, defined by the geometrical defocusing, of at least 5000 in the whole selected spectral range with VLS grating operational width of 50 mm, and the resolving power, conditioned by higher-order aberrations, of more than 1000 in the whole range.

Let's start with a more short-wave range of 125–1000 Å, for which the grooves frequency in the center of the VLS grating is already defined as $p_0 = 600 \text{ mm}^{-1}$, angle of the radiation deflection by the grating is $\Omega = 32^\circ$, distance from the grating center to the exit slit is $L_2 = 1200 \text{ mm}$, the range is 125–1000 Å, the width of the VLS grating is 50 mm, the distance from the grating center to the focusing mirror center is 150 mm. To maximize the minimum resolving power in the whole range we select $\lambda_1 = 200 \text{ Å}$ and $\lambda_2 = 770 \text{ Å}$ as the wavelengths $\lambda_{1,2}$ of the rigorous focusing. To achieve that, the distance from the grating center to the focus of the convergent beam incident onto the grating, $L_1 \approx 1201.65 \text{ mm}$ is required, as well as $p_1 = 0.956 \text{ mm}^{-2}$. To provide such a beam incident onto the grating, the auxiliary focusing mirror should have the following parameters: distance from the source to

the mirror — 28000 mm, distance from the mirror to the grating — 150 mm, mirror grazing-incidence angle — 16° , mirror curve radius — 9356 mm.

The distance from the diffracted radiation focus to the exit slit will change from zero to less than 4.5 mm in the whole range, while the image width, conditioned by the geometrical defocusing, will be less than $20 \mu\text{m}$ in a range of 100–850 Å. The plate scale changes from 3.6 Å/mm at 120 Å to 2.35 Å/mm at 1000 Å, while resolving power will be more than 5000 in the whole spectral range (Fig. 3).

To evaluate the image width, conditioned by higher-order aberrations, the numerical ray tracing of the scheme was performed using XOP 2.3 software with SHADOW VUI 1.12 extension [28]. If VLS grating coefficient is $p_2 = 0$, the coma will be the defining aberration, due to which the image width will be equal to fractions of 1 mm. For its compensation the parameter p_2 should be selected. The optimization criteria is the requirement for the resolving power R to be at least 1000 in the whole range. However, if examining $R = \lambda/\Delta\lambda$, using the full (to base) image width as $\Delta\lambda$, then, by selecting $p_2 = -1.50 \cdot 10^{-3} \text{ mm}^{-3}$, we obtain $R = 1000–1400$. The image width in the whole range is still defined by coma, therefore we can increase R twice by reducing the grating width by 1.5.

When transitioned to the long-wave range of 900–4200 Å with a grating with $p_0 = 150 \text{ mm}^{-1}$, the angle of radiation deflection by the grating $\Omega = 32^\circ$, the distance from the

grating center to the exit slit $L_2 = 1200$ mm, the distance from the grating center to the focus of the incident onto the grating convergent beam $L_1 \approx 1201.65$ m, grating width of 50 mm, as well as parameters of grazing-incidence focusing mirror remain unchanged. Coefficient p_1 , that will define the fine focusing wavelengths λ_1 and λ_2 , remains the free parameter. In this case, since parameter L_1 is already defined, at maximizing the minimum resolving power in the whole range, one of the points goes out of the range: $p_1 = 0.24 \text{ mm}^{-2}$, $\lambda_1 = 726 \text{ \AA}$ and $\lambda_2 = 3290 \text{ \AA}$.

Parameters, conditioned by geometrical defocusing, will be as follows: image width will be less than $40 \mu\text{m}$ in a range of $900\text{--}3800 \text{ \AA}$, defocusing (distance from diffracted radiation focus to the exit slit) will be less than 5 mm for all wavelengths from the examined spectrum range, the plate scale from 14.0 \AA/mm at 900 \AA to 9.1 \AA/mm at 4200 \AA . Calculated resolving power is more than 5000 in the whole spectral range (Fig. 3).

To evaluate the image width, conditioned by higher-order aberrations, the numerical ray tracing was also performed. By selecting $p_2 = -1.40 \cdot 10^{-4} \text{ mm}^{-3}$, we obtain values $R > 2000$ in the whole spectral range of $900\text{--}4200 \text{ \AA}$ (Fig. 4).

General parameters of the calculated scheme of VLS monochromator are presented in the table.

Conclusion

A project of a high-resolution monochromator for the spectral range of $125\text{--}4200 \text{ \AA}$ is calculated for use at an end station measuring channel of the new Siberian 4th generation synchrotron „SKIF“ („The Siberian ring source of photons“). A monochromator based on the Hettrick–Underwood scheme uses a concave focusing mirror and two replaceable VLS gratings. The wavelengths scanning is performed by solely the grating rotation at a constant direction of the output radiation. Aberrations of the grazing-incidence mirror, installed in a strongly asymmetrical scheme, are suppressed by the VLS grating. The monochromator can provide a resolving power of more than 1000 in the range of $125\text{--}1000 \text{ \AA}$ and above 2000 in the range of $900\text{--}4200 \text{ \AA}$.

Funding

The study is performed under the partial grant support of the Ministry of Science and Higher Education of the Russian Federation №075-15-2020-781.

Conflict of interest

The authors declare that they have no conflict of interest.

References

- [1] A.V. Bukhtiyarov, V.I. Bukhtiyarov, A.D. Nikolenko, I.P. Prosvirin, R.I. Kvon, O.E. Tereshchenko. AIP Conf. Proc., **2299**, 060003 (2020). DOI: 10.1063/5.0030740
- [2] W.R. Hunter, R.T. Williams, J.C. Rife, J.P. Kirkland, M.N. Kabler. Nucl. Instrum. Meth., **195**, 141 (1982). DOI: 10.1016/0029-554X(82)90768-6.
- [3] M.C. Hettrick, J.H. Underwood. AIP Conf. Proc., **147**, 237 (1986). DOI: 10.1063/1.35993.
- [4] M.C. Hettrick, J.H. Underwood, P. Batson, M. Eckart. Appl. Opt., **27** (2), 200 (1988). DOI: 10.1364/AO.27.000200
- [5] P. Miotti, N. Fabris, F. Frassetto, C. Spezzani, L. Poletto. AIP Conf. Proc., **2054**, 060023 (2019); DOI: 10.1063/1.5084654.
- [6] E.A. Vishnyakov, A.O. Kolesnikov, A.S. Pirozhkov, E.N. Ragozin, A.N. Shatokhin. Quant. Electron., **48** (10), 916 (2018) [E.A. Vishnyakov, A.O. Kolesnikov, A.S. Pirozhkov, E.N. Ragozin, A.N. Shatokhin. Quant. Electron., **48** (10), 916 (2018)]. DOI: 10.1070/QEL16707
- [7] E.N. Ragozin, E.A. Vishnyakov, A.O. Kolesnikov, A.S. Pirozhkov, A.N. Shatokhin. Phys. Usp., **191** (5), 522 (2021). [E.N. Ragozin, E.A. Vishnyakov, A.O. Kolesnikov, A.S. Pirozhkov, A.N. Shatokhin. Phys. Usp., **191** (5), 522 (2021). DOI: 10.3367/UFNe.2020.06.038799]
- [8] J. Dunn, E.W. Magee, R. Shepherd, H. Chen, S.B. Hansen, S.J. Moon, G.V. Brown, M.-F. Gu, P. Beiersdorfer, M.A. Purvis. Rev. Sci. Instrum., **79**, 10E314 (2008). DOI: 10.1063/1.2968704
- [9] T. Harada, H. Sakuma, K. Takahashi, T. Watanabe, H. Hara, T. Kita. Appl. Opt., **37** (28), 6803 (1998). DOI: 10.1364/AO.37.006803
- [10] M.C. Hettrick, S. Bowyer. Appl. Opt., **22** (24), 3921 (1983). DOI: 10.1364/AO.22.003921
- [11] M.C. Hettrick, S. Bowyer, R.F. Malina, C. Martin, S. Mrowka. Appl. Opt. **24** (12), 1737 (1985). DOI: 10.1364/AO.24.001737
- [12] A. Miyake, T. Miyachi, M. Amemiya, T. Hasegawa, N. Ogushi, T. Yamamoto, F. Masaki, Y. Watanabe. Proc. SPIE, **5037**, 647 (2003). DOI: 10.1117/12.484969
- [13] M. Terauchi, S. Koshiya, F. Satoh, H. Takahashi, N. Handa, T. Murano, M. Koike, T. Imazono, M. Koeda, T. Nagano, H. Sasai, Y. Oue, Z. Yonezawa, S. Kuramoto. Microsc. Microanal., **20**, 692 (2014). DOI: 10.1017/S1431927614000439
- [14] J.H. Underwood, E.M. Gullikson, M. Koike, S. Mrowka. Proc. SPIE, **3150**, 40 (1997). DOI: 10.1117/12.292734
- [15] J.-J. Wang, Y.E. Mao, T. Shi, R. Chang, S. Qiao. Chin. Phys. C, **39** (4), 048001 (2015).
- [16] L. Du, X. Du, Q. Wang, J. Zhong. Nucl. Instrum. Meth. A, **877**, 65 (2018). DOI: 10.1016/j.nima.2017.09.045
- [17] O. Fuchs, L. Weinhardt, M. Blum, M. Weigand, E. Umbach, M. Bär, C. Heske, J. Denlinger, Y.-D. Chuang, W. McKinney, Z. Hussain, E. Gullikson, M. Jones, P. Batson, B. Nelles, R. Follath. Rev. Sci. Instrum., **80**, 063103 (2009). DOI: 10.1063/1.3133704
- [18] T. Warwick, Y.-D. Chuang, D.L. Voronov, H.A. Padmore. J. Synchrotron Radiat., **21**, 736 (2014). DOI: 10.1107/S1600577514009692
- [19] J. Dvorak, I. Jarrige, V. Bisogni, S. Coburn, W. Leonhardt. Rev. Sci. Instrum., **87**, 115109 (2016). DOI: 10.1063/1.4964847
- [20] M.A. Cornu. Comptes Rendus Acad. Sci., **117**, 1032 (1893).

- [21] T. Harada, S. Moriyama, T. Kita. *Jpn. J. Appl. Phys.*, **14** (51), 175 (1975). DOI:10.7567/JJAPS.14S1.175
- [22] T. Harada, T. Kita. *Appl. Opt.*, **19** (23), 3987 (1980). DOI: 10.1364/AO.19.003987
- [23] T. Kita, T. Harada. *Appl. Opt.*, **31** (10), 1399 (1992). DOI: 10.1364/AO.31.001399
- [24] T. Kita, T. Harada, N. Nakano, H. Kuroda. *Appl. Opt.*, **22** (4), 512 (1983). DOI: 10.1364/AO.22.000512
- [25] Hettrick Scientific [Electronic source] Available at: <http://hettrickscientific.com/>
- [26] A.O. Kolesnikov, E.A. Vishnyakov, A.N. Shatokhin, E.N. Ragozin. *Quant. Electron.*, **49** (11), 1054 (2019). [A.O. Kolesnikov, E.A. Vishnyakov, A.N. Shatokhin, E.N. Ragozin. *Quant. Electron.*, **49** (11), 1054 (2019). DOI: 10.1070/QEL17074]
- [27] A.N. Shatokhin, A.O. Kolesnikov, P.V. Sasorov, E.A. Vishnyakov, E.N. Ragozin. *Opt. Express*, **26** (15), 19009 (2018). DOI: 10.1364/OE.26.019009
- [28] ESRF. XOP (X-ray Oriented Programs) [Electronic source] Available at: <https://www.esrf.fr/Instrumentation/software/data-analysis/xop2.3>